Passive Human Motion Detection using Wi-Fi Sensing

Koidala Surya Prakash, Vedala Sai Ashok and Chintha Pranay Prakash

I. INTRODUCTION

Device free passive detection is an emerging technology to detect the presence of humans in the target environment without any devices attached to them. It is an essential primitive for various real life applications like intrusion detection, patient monitoring in hospitals, child and elder care in the home and battlefield military operations.In such applications, users should not be expected to carry any purposed devices for localization or detection. Consequently, traditional device-based techniques that require specialized hardware attached to people are no longer applicable.

With the widespread development and deployment of wireless networks, it is possible to realize passive detection of humans by capturing the wireless context changes caused by them. Various moralities of radio signals have been explored to enable device-free passive detection, among which RSS is one of the most popular ones due to its handy accessibility on existing wireless infrastructure. RSS based device-free detection schemes exploit variations in RSS measurements to infer anomalous environment changes. RSS based scheme still suffers from high susceptibility to background noise. As a result false detection can happen frequently in a scheme utilizing RSS.

More robust and reliable solutions resort to using Channel State Information(CSI) which is more sensitive to human presence and more stable in static environments. Channel State Information (CSI), which is now tractable on commodity network interface cards (NICs), presents sub-carrier-level channel measurements in the framework of the modern OFDM technique. In this article we have used both amplitude and sensitive phase information of CSI for passive human detection.

II. PRELIMINARIES

A. Channel State Information (CSI)

Orthogonal Frequency Division Multiplexing(OFDM) is a bandwidth efficient digital multi-carrier modulation scheme, which has been widely adopted in many modern wireless communication systems. In OFDM, signals are transmitted over many orthogonal frequencies called subcarriers. Based on OFDM CSI describes how a signal propagates from the transmitter to the receiver at the subcarrier level, revealing the combined effect of, for instance reflecting,scattering and power decay with distance. With slight driver modification on off-the-shelf NIC, e.g., Intel 5300, CSI can be exported to the upper users on N=30 subcarriers.

$$H = |H(f_1), H(f_2), ..., H(f_i)|, i\epsilon|1, N| \quad (1)$$

where $H(f_i)$ is the CSI at subcarrier i with central frequency f_i. Each CSI $H(f_i)$ depicts the amplitude and phase of OFDM subcarrier i:

$$H(f_i) = |H(f_i)|e^{j\angle H(f_i)} \quad (2)$$

Here $|H(f_i)|$ and $\angle H(f_i)$ represent amplitude and phase, respectively.

B. MIMO

The use of multiple antennas at the transmitter and receiver has revolutionized wireless communication over the past decade. MIMO uses multiple antennas to increase the reliability via spatial diversity and improve the data throughput via spatial multiplexing without enhancing the bandwidth and transmission power. Since there are multiple antennas in MIMO, each combination of transmitter and receiver antenna can be considered as a separate TX-RX data stream. Suppose there are m transmit antennas and n receive antennas, the CSI of all TX-RX data streams can be expressed as:

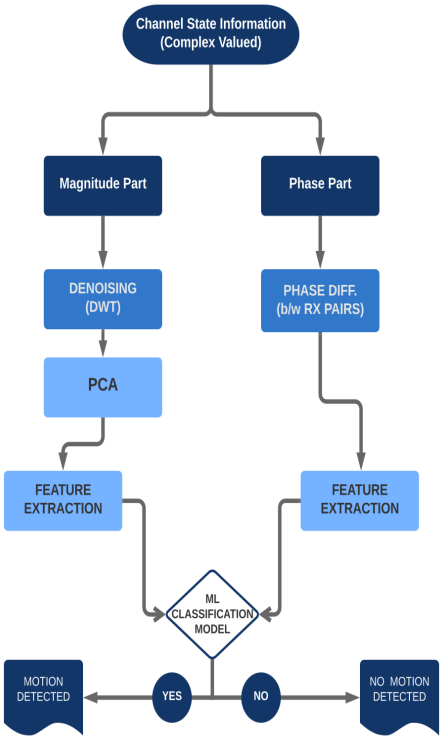

Fig. 1. Flowchart

$$\begin{bmatrix} H_{11} & H_{12} & \dots & H_{1n} \\ H_{21} & H_{22} & \dots & H_{2n} \\ \vdots & \vdots & \ddots & \dots \\ H_{m1} & H_{m2} & \dots & H_{mn} \end{bmatrix} \tag{3}$$

where H_{mn} is a vector describing the CSI of all subcarriers between the m-th transmit antenna to the n-th receive antenna.

III. OVERVIEW

Fig.1 shows a brief description of procedures in a flowchart.

IV. METHODOLOGY

A. Data Preprocessing

Leveraging the off-the-shelf NIC with slight driver modification, a group of CFRs on N=30 subcarriers can be exported to up-layer users for every one packet in the format of CSI:

$$H = [H(f_1), H(f_2), ..., H(f_N)] \tag{4}$$

Each CSI represents amplitude and phase of an OFDM subcarrier:

$$H(f_k) = |H(f_k)|e^{j\angle H(f_k)} \tag{5}$$

where $H(f_k)$ is the CSI at the subcarrier k($k\epsilon[1, 30]$) with central frequency off_k, and $\angle H(f_k)$ denotes its phase. To monitoring an area of interest, CSIs are continously collected and K measurements within a specefic time window form the CSI sequence, which can be denoted as

$$H = [H_1, H_2, ..., H_K] \tag{6}$$

The K measurements of CFR then serve as the basic input for our movement detection algorithm. These K measurements of CFR values are parsed and downsampled to create CFR of 300 measurements across 3 receivers consisting of 30 subcarriers each. The amplitude and phase information of these CFR measurements are separated, which will first be preprocessed and then features are extracted from these measurements.

B. Amplitude preprocessing

1) DENOISING: We consider each column from the dataset which corresponds to a time series data related to a single subcarrier and perform DWT (Discrete Wavelet Transform).

DWT outperforms the Fourier Transform in case of non-stationary signal , which is the case here. Also it is not appropriate to use a conventional filter, such as Butterworth filter since the passband for the low-pass filter usually needs to be less than one-twentieth of the sampling rate, so that the energy of the residual noise in the passband becomes negligible compared to the signal energy [1].

The collected CSI samples are noisy due to commercial Wifi devices are susceptible to complex indoor environment.

Therefore the time series of each Sub-Carrier involves high frequency noise . Hence we apply the wavelet based denoising scheme to remove random noise and smooth out CSI data.

Wavelet denoising consists of 3 stages : decomposition , thresholding , reconstruction .

During the decomposition procedure, discrete wavelet transform recursively splits into two parts, high frequency coefficients (details) and low frequency coefficients (approximations), at different frequency levels.

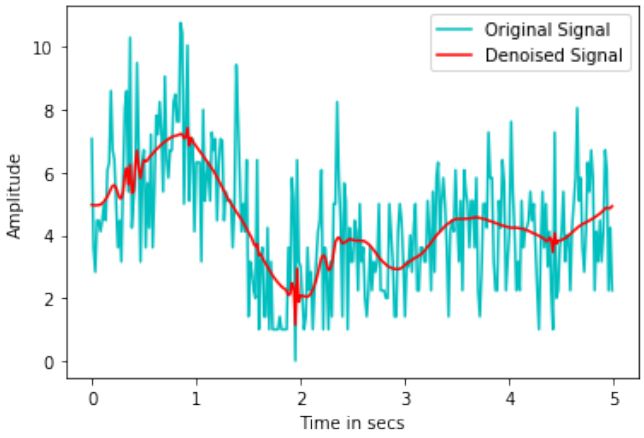

Fig. 2. Demonstrating the denoising scheme using **DWT**

Thresholding is applied to the high frequency parts thereby decreasing the contribution of high frequency parts.

Finally, we reconstruct the denoised signal by combining the approximation coefficient of the last level with thresholded details.

Fig 2 illustrates how the DWT can knockout high-frequency noise.

C. Phase Sanitization

Due to random noise and an unsynchronized time clock between transmitter and receiver, raw phase information behaves extremely randomly making it inapplicable for any detection.

Let $\hat{\phi}_i$ denote the measured phase of subcarrier i, which is given by

$$\hat{\phi}_i = \phi_i + (\lambda_p + \lambda_s)m_i + \lambda_c + \beta + Z \qquad (7)$$

where ϕ_i is the true phase, m_i is the subcarrier index of subcarrier i , β is the initial phase offset due to the phase-locked loop, Z is the measurement nose that is assumed to be AWGN of variance σ^2, and λ_p, λ_s and λ_c are the phase errors from the packet boundary detection(PBD), the sampling frequency(SFO) and central frequency offset(CFO), respectively.

$$\lambda_p = 2\pi\frac{\Delta t}{N}$$

$$\lambda_s = 2\pi\frac{T' - T}{T}\frac{T_s}{T_u} \qquad (8)$$

$$\lambda_c = 2\pi\Delta f T_s n$$

where Δt is the packet boundary detection delay, N is the FFT size, $T'$and T are the sampling periods at the receiver and the transmitter, respectively, T_u is the length of the data symbol, T_s is the total length of a data symbol and the guard interval, n is the sampling time offset for the current packet, and Δf is the center frequency difference between the transmitter and receiver.

We cannot obtain the exact values for Δt, $\frac{T'-T}{T}$, n, Δf and β in the equation mentioned in the 8.So true phase cannot be derived from the measured phase value and thus measured phase cannot be used directly for detection as it is not stable.But the measured phase difference on subcarrier i between two receiver antennas is stable.The three antennas of the Intel 5300 NIC use the same clock and the same down converter frequency. Consequently, the measured phases from two antennas have identical packet detection delay, sampling periods, frequency differences and the same index. Measured phase difference on subcarrier i between two antennas can be approximated as

$$\Delta\hat{\phi}_i = \Delta\phi_i + \Delta\beta \qquad (9)$$

Since Δt , Δf and n are all removed, $\Delta\hat{\phi}_i$ becomes highly stable for consecutive packets. It can also be seen that E($\Delta\hat{\phi}_i$) - E($\Delta\phi_i$) is a constant β.

D. Feature Extraction

An appropriate feature plays a crucial role in device-free detection, and feature extraction as most important component. Various statistical features have been explored for detection, such as variance, IQR, mean and so forth. But the feature metric selected should be absolute power irrelevant and possibly variance dependent, since transmitting power parameters would be adapted over different scenarios and thus are scenario dependent.

Variances of both amplitude and phase in cases when human movements are significantly larger than those in static cases. But due to lack of knowledge on transmit power at the receiver side, variance cannot be normalized to adapt to diverse scenarios and thus cannot be directly used for human detection.

As a consequence, we have extracted the features from respective correlation matrix of CFR amplitude and phase of 300 sequential measurements over a certain time window.

1) Amplitude: To discover the correlations between subcarriers, we choose to conduct principal component analysis on each CSI stream to unveil the most common variations among different subcarriers. PCA is perfomed on the CSI amplitude time series resulting from wavelet filtering. Denote $H_{t,r}(i)$ as the N*1 dimension vector representing the CSI amplitude values of the N= 30 subcarriers between a TX-RX antenna pair t-r for the i^{th} CSI sample. Then, let $H_{t,r}$ be a K*N dimension matrix containing the CSI amplitude values of N subcarriers between a TX-RX antenna pair t-r for K consecutive samples.

$$H_{t,r} = [H_{t,r}(1), H_{t,r}(2), H_{t,r}(3), ...H_{t,r}(K)]^T \tag{10}$$

Each column of the matrix $H_{t,r}$ represents the CSI amplitude time series for one OFDM subcarrier for K consecutive measurements. Then standardise the matrix $H_{t,r}$ so that each column has zero mean and unit variance, denoted as $Z_{t,r}$.

$$Z_{t,r} = [Z_{t,r}(1), Z_{t,r}(2), Z_{t,r}(3), ...Z_{t,r}(K)]^T \tag{11}$$

Calculate the corresponding correlation matrix for $Z_{t,r}$

$$\begin{bmatrix} C(1,1) & C(1,2) & \dots & C(1,N) \\ C(2,1) & C(2,2) & \dots & C(2,N) \\ \vdots & \vdots & \ddots & \dots \\ C(N,1) & C(N,1) & \dots & C(N,N) \end{bmatrix} \tag{12}$$

where each element C(i,j) denotes the correlation coefficient between $Z_{t,r}(i)$ and $Z_{t,r}(j)$.

After computing the correlation matrix, we perform eigendecomposition of the correlation matrix to obtain eigenvectors $E = (e_1, e_2, e_3, ..., e_i)$.

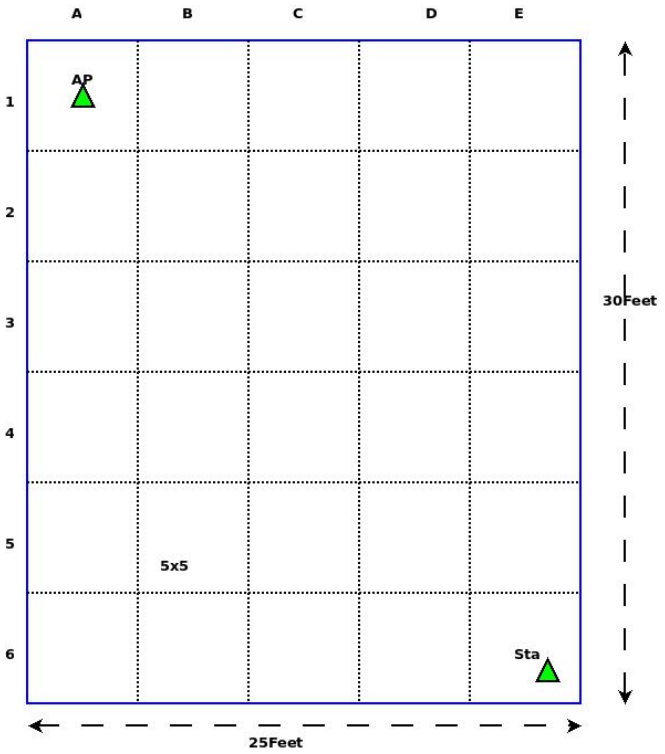

Fig. 3. Single Room

To obtain a robust feature for human detection, we analyze the eigenvectors. We observe that eigenvectors vary randomly across neighbouring subcarriers in human-free scenario, whereas they fluctuate more smoothly in the presence of human movement. Based on these observation, we can calculate the mean of first-order difference of eigenvectors as

$$Diffe_i = \frac{1}{N-1} \sum_{k=2}^{N} |e_i(k) - e_i(k-1)| \tag{13}$$

where N=30 is the number of subcarriers and $|e_i(k) - e_i(k-1)|$ is the difference between neighbouring subcarriers of the i^{th} eigenvector. The above mentioned $Diffe_1$,$Diffe_2$,$Diffe_3$ and $Diffe_4$ are used as input features for classification.

2) Phase: For extracting features from phase information of CSI we perform PCA on phase information of each CSI stream to unveil the most common variations among different subcarriers. PCA is performed on the CSI phase time series resulting from phase difference. We first standard-

ise these phase CSI streams and calculate their corresponding covariance matrix.

$$C(\phi) = [C(\phi_i, \phi_j)]_{KxK} \tag{14}$$

where $C(X_i, X_j)$ denotes the correlation between vectors X_i and X_j.

To extract a simple feature for detection using CSI phase information, we compute the eigenvalues of CSI phase correlation matrix and select the maximum eigenvalue of the correlation matrix.

$$\alpha = max(eigen(C(\phi))) \tag{15}$$

In order to guarantee the accuracy and robustness of detection, we further introduce the second maximum eigenvalue of CSI phase information.

V. DATASET DESCRIPTION

Each data point consists of CSI values recorded by INTEL NIC 5100

- A recording lasts for 5 sec being sampled at 60 Hz.
- An average human moves at a 1m/sec in a room, it will lead to a 10 Hz Doppler Shift. This shift leads to a change in phase by $2\pi f_C t_S$.The finer the t_S , the better resolution of change is observed.
- Hence so as to capture this change in consecutive samples , a 60 Hz sampling rate is sufficient.
- Hence a data point consists of 300 time samples each with 90 columns (3x30) , i.e, 3 receivers and 30 subcarriers.

A. Dataset description

The data is collected in 2 forms:

- Static data: no movement
- Dynamic data :Individuals are moving.

Now, that we have a raw dataset. Each datapoint comprises of a (300 x 90) matrix. Where,

90 $\rightarrow$ no. of columns ; which is (3Rx x 30 subcarriers)

300 $\rightarrow$ time samples (5sec x 60Hz)

This datapoint is considered and preprocessed as shown in the flowchart.

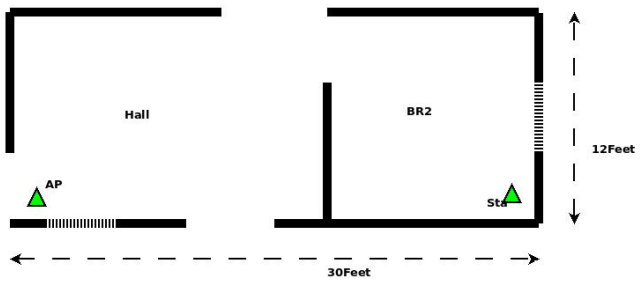

Fig. 4. 1 BHK

VI. EXPERIMENTS AND EVALUATION

A. Implementation

The dataset has been collected by wifi commodity devices.The Tx has been set to operate in AP mode. the Rx is equipped with INTEL 5300 NIC .

- During the experiment the receiver pings packets from the router at a rate of 1KHz packets/sec, and records CSI from each packet.
- A recording lasts upto 30 sec.
- We later downsampled and performed timeparsing so as to enhance the dataset for better learning.

P.S : The above implementation has been performed by the company - 'GYRUS' and was provided to us.

B. Environment

Similar experiments have been performed in 3 different indoor environments to learn about the effect of surroundings.

- A Single Room : Here a Tx and a Rx are arranged at the diagonal corners and people are made to move in the room. Please refer Fig 3 for the layout.
- A 1BHK flat : Here a Tx and Rx are placed in different rooms which are divided by a wall. Please refer Fig 4 for the layout.
- A 2BHK flat : This is the same as the previous scenario, rather we have more rooms here and recordings are recorded in every room. Please refer Fig 5 for the layout.

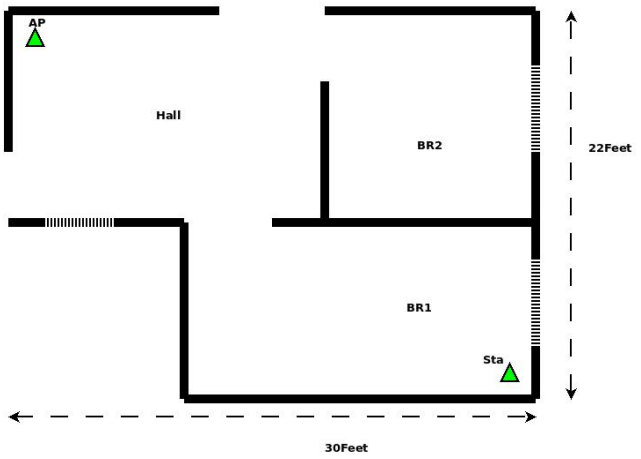

Fig. 5. 2 BHK

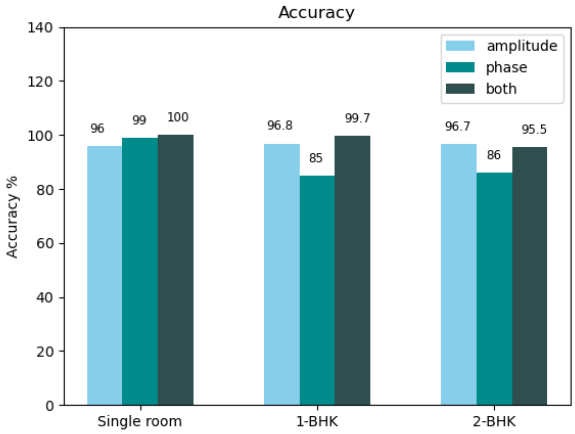

Fig. 6. Accuracy for different environments

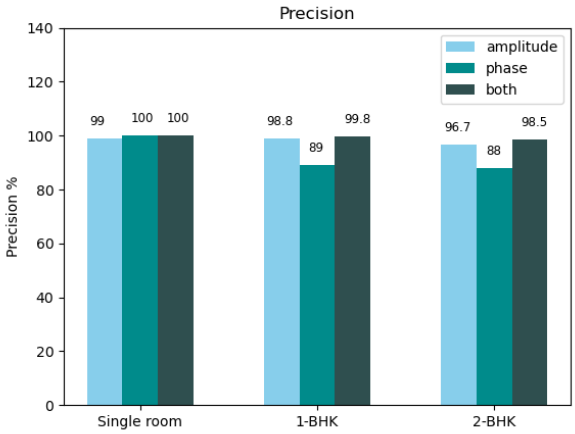

Fig. 7. Precision for different environments

VII. EVALUATION

A. Machine Learning Model

Since they are few features which are obtained through feature extraction. We landed up using SVM(Support Vector Machine) model for classification. We evaluated the model using features derived from the amplitude part , features derived from the phase part and also obtained some hybrid features which is derived from both the amplitude and the phase part- this is termed as all in the histogram.

B. EVALUATION METRICS

We chose Accuracy and Precision to be metrics for evaluations. The results are portrayed in the form of histograms.

VIII. OBSERVATIONS

- The first environment has a LOS(Line of Sight) path since there are no obstacles between the Tx and Rx . While the latter environments are arranged in a NLOS path . There is no direct LOS path between them in these cases.
- Hence due to this the signals tend to reflect more from the walls , which leads to more multipaths in the NLOS cases.
- The Single room environment has a direct LOS path from Rx to Tx , hence there will be less multipaths here, and adding to that a human obstructing the LOS path acts as a obstacle (like a wall) and thus the signal bounces of from there as well. Hence we were able to predict the result better in this case , rather than other cases.
- The phase feature although was not much of a help here , but usually consists information about finer changes. Hence it is usually used for detecting small scale action like breathing etc;

IX. ACKNOWLEDGMENT

We cannot express enough thanks to our supervisor , **Dr. Sai Dhiraj Amuru** for his continued support and encouragement throughout the course of this project.
We also thank **GYRUS**,the company to offer data which has been a major source to the project.

REFERENCES

[1] R-TTWD: Robust Device-free Through-The-WallDetection of Moving Human with WiFi, Hai Zhu, Fu Xiao, Lijuan Sun, Ruchuan Wang, and Panlong Yang

[2] Enabling Contactless Detection of Moving Humanswith Dynamic Speeds Using CSI, KUN QIAN, CHENSHU WU, ZHENG YANG, and YUNHAO LIU,FUGUI HE,TIANZHANG XING.

[3] Poster: Crowdsourced Location Aware Wi-Fi Access Control

[4] Multi-Target Intense Human Motion Analysis and Detection Using Channel State Information †

[5] Device-Free User Authentication, Activity Classification and Tracking using Passive Wi-Fi Sensing: A Deep Learning Based Approach

[6] Wi-Multi: A Three-Phase System for Multiple Human Activity Recognition With Commercial WiFi Devices

[7] Human Activity Sensing with Wireless Signals: A Survey

[8] SEARE: A System for Exercise Activity Recognition and Quality Evaluation Based on Green Sensing Fu Xiao, Member, IEEE, Jing Chen, Xiaohui Xie, Linqing Gui, Lijuan Sun, and Ruchuan Wang

[9] Anti-fall: A Non-intrusive and Real-Time Fall Detector Leveraging CSI from Commodity WiFi Devices

[10] WiFi-Based Real-Time Calibration-Free Passive Human Motion Detection †

[11] Non-invasive Detection of Moving and Stationary Human with WiFi

[12] WiHACS: Leveraging WiFi for Human Activity Classification using OFDM Subcarriers' correlation

[13] Electronic Frog Eye: Counting Crowd Using WiFi